Influence of non-stationary content of ground-motions on nonlinear dynamic response of RC bridge piers

Mohammad M Kashani[1], Christian Málaga-Chuquitaype [2], Shijia Yang[2] Nicholas A Alexander[3]

Abstract

This paper quantifies the impact of the non-stationary content (time-varying parameters that are not captured by power spectral content alone) of different ground-motion types (near/far field, with/without pulses time-series) on the nonlinear dynamic response of reinforced concrete (RC) bridge piers, taking into account the material cyclic degradation. Three groups of ground motions are selected to represent far-field, near-field without pulse and near-field pulse-like ground motions. Three analysis cases are considered corresponding to acceleration series matched to the mean response spectrum of: (*i*) far field, (*ii*) near-field without pulse and (*iii*) near-field pulse-like ground-motions, respectively. Using the selected ground motions, several nonlinear incremental dynamic analyses (IDAs) of prototype reinforced concrete bridge piers with a range of fundamental periods are conducted. Finally, a comparison between the response of the structures using the material model accounting for both buckling and low-cycle fatigue of reinforcing steel and the more conventional material model that does not account for these effects is made. The results show that the inelastic buckling and low-cycle fatigue have a significant influence on the nonlinear response of the RC bridge piers considered and that pulse effects can increase the mean acceleration response by about 50%.

Keywords: Incremental dynamic analysis, low-cycle fatigue, response spectrum matching, ground-motion duration, nonlinear analysis, inelastic buckling

1. Introduction

The current state-of-the-practice and modern seismic design codes (Eurocode 8 2010, Caltrans 2013) rely on a proper detailing of the plastic hinge regions where most of the inelastic deformations are expected to occur. Therefore, the structural performance is greatly influenced by the structural details (e.g. sufficient confinement for concrete) and material performance (e.g. ductility of reinforcing steel). Furthermore, given that earthquakes are an extreme cyclic dynamic loading case, they result in significant tension and compression strain reversals at critical cross sections in the plastic hinge regions. This subsequently leads to low-cycle high-amplitude fatigue degradation on materials (Kunnath et al. 1997, Mander at al. 1994, Chang and Mander 1994, Kashani 2014). Bridge piers are the most important and critical elements in bridges due to the nature of their structural system. Unlike building structures, where plastic hinges typically initiate in beams, in bridges, plastic hinges only occur in piers with the deck remaining elastic. Therefore, bridge piers must sustain very large inelastic deformations without collapsing during seismic events to dissipate energy. The combined effects of the large lateral deformation and axial force in bridge piers can induce inelastic buckling of vertical reinforcement which subsequently results in crushing of core confined concrete (Lehman and Moehle 2000, Berry and Eberhard 2003, Kashani 2014). Kashani et al. (2015a,b) reported that inelastic buckling of reinforcing bars has a significant impact on the reduction of their low-cycle high-amplitude fatigue life. Furthermore, they found that the low-cycle fatigue failure of reinforcement has a significant load-path dependency. Therefore, it is very important to account for the influence of material degradation under seismic loading in performance prediction of reinforced concrete (RC) bridge piers using nonlinear dynamic analysis.

[1]University of Southampton, Faculty of Engineering and the Environment, and University of Bristol, Dept. of Civil Engineering, UK (corresponding author), Email: mehdi.kashani@soton.ac.uk
[2]Imperial College London, Dept. of Civil and Environmental Engineering, UK
[3]University of Bristol, Dept. of Civil Engineering, Bristol, UK

Furthermore, characterising, by a few salient parameters, the influence of a particular ground-motion time-series, on the nonlinear response of some structural systems is a vexed problem. Engineers and seismologists have employed a range of amplitude, energy, averaged frequency content, duration and envelope shape measures etc. (Málaga-Chuquitaype 2015, Sarieddine and Lin 2013, Cornell 1997, Hancock and Bommer 2007, Iervolino et al. 2006, Raghunandan and Liel 2013, Kramer 1996) to attempt to capture the most significant factors that govern the nonlinear response of the system. In particular, if we consider near/far field, with/without pulses, time-series it is immediately apparent that there are differences. These differences are expressed in their power spectral content which describes the averaged-temporally components of the time-series which are statistically stationary (Chatfield 2003). The elastic response spectrum represents a smoothed and filtered estimate of the power spectral content of the time-series. They could be fully described by a proper Fourier spectral approach that includes both power and phase spectral content. Unfortunately phase spectral content is difficult to interpret. Hence the elastic response spectra are employed by seismologists and engineers as a proxy for power spectral content. Besides, there are also differences in near/far field, with/without pulses, time-series caused by the non-stationary statistical content which are not captured by power spectral content alone (Li et al. 2016). This non-stationary (time-varying) statistical content (Chatfield 2003) includes the envelope shape and the presence of large, time localised, pulses in the ground-motion time-series.

Hancock and Bommer (2006) summarised previous studies and reported that the conclusions are greatly influenced by which structural demand parameters are considered. For example, comparing the responses to spectrally compatible far-field and short near-field pulse-like ground motions may not yield significant differences in the maximum peak drift demands. However, given that the far-field ground motions are normally longer they will affect the accumulated damage on the structure due to low-cycle high-amplitude fatigue degradation of materials (Kunnath 1997, Hancock and Bommer 2004, Hancock and Bommer 2007). Current seismic design codes and loading protocols for component testing of structural components do not account for the influence of ground-motion characteristics i.e. duration, pulse effect etc. In recent years, new standards such as ASCE (2010), FEMA (2012) and PEER (2010) provide some guidelines to account for the ground-motion duration qualitatively. However, they do not have a well-defined framework for quantifying and accounting for the ground-motion characteristics.

A recent study conducted by Chandramohan et al. (2015), proposes a methodology to quantify the effect of ground-motion duration on the probability of structural collapse. In order to isolate the effect of duration from other ground-motion characteristics, such as amplitude and frequency content, they used spectrally equivalent, long and short duration record sets, with unmodified spectral content. Cyclic deterioration of the structural component is implicitly considered via a lumped-plasticity model for a single bridge pier using the Ibarra et al. (2005) model. It should be noted that prior to Chandramohan et al. (2015), none of the earlier numerical studies accounted for the effect of cyclic deterioration in the nonlinear structural models (Sarieddine and Lin 2013, Cornell 1997, Hancock and Bommer 2007, Iervolino et al. 2006, and Raghunandan and Liel 2013). However, the Ibarra et al. (2005) model that is employed in the Chandramohan et al. (2015) study, does not account for cross section geometry and axial force-bending moment interaction of RC sections and components. Furthermore, this model has to be calibrated for a specific cross section geometry, reinforcement arrangement and axial force ratio. Therefore, it is unable to capture the influence of the loading spatiotemporal history on the failure mode and cannot predict the multiplicity of failure modes. Subsequently, the true correlation between the ground-motion type such as far-field ground motions and near-field (with/without pulse) and the nonlinear dynamic response of RC bridge piers has not been quantified in any of the previous studies and remains to be fully appraised.

Accordingly, the aim of this paper is to develop a novel approach to quantify the impact of ground-motion types (near/far field, with/without pulses time-series), caused by the non-stationary content (time-varying parameters that are not captured by power spectral content alone), on the nonlinear dynamic response of RC bridge piers taking into account the material cyclic degradation. This paper

determines the effect of near/far field, with/without pulses, time-series on the nonlinear dynamic responses of structural systems by separating out the influence of the stationary and non-stationary components.

With this in mind, the new algorithm (known as RVSA) developed by Alexander et al. (2014) is employed to generate a set of artificial ground motions of equivalent spectral response. The ground-motion seeds are selected from the suggested far-field (FF), near-field without pulse (NFWP) and near-field pulse like (NFPL) ground motions in FEMA P695 (2009). These ground motions have differences in amplitude, duration and power spectral content, i.e. differences in stationary and non-stationary components. Then, using the RVSA they are all matched to a target response spectrum (without qualitatively changing the non-stationary ground-motion characteristics, i.e. envelope and pulses) to be used in nonlinear dynamic analyses. This will isolate the influence of ground-motion envelope and pulses (non-stationary effects) from ground-motion response spectral characteristics (stationary effects). Here three sets of matched ground-motion cases are considered:

• Case I, all ground motions are modified (using RVSA) such that each of their response spectra matches the mean response spectrum of the FF ground-motion group.

• Case II, all ground motions are modified (using RVSA) such that each of their response spectra matches the mean response spectrum of the NFWP ground-motion group.

• Case III, all ground motions are modified (using RVSA) such that each of their response spectra matches the mean response spectrum of the NFPL ground-motion group.

In each of the three cases I, II, and III there are three sub-cases with different ((a) FF, (b) NFWP and (c) NFPL) non-stationary components. Therefore, nine different cases are explored. Thus, for example, case II contain records with nearly identical stationary components (that are the mean of the NFWP group) but different nonstationary components (seeds from FF, NFWP and NFPL).

The nonlinear finite element model employed in this study incorporates an advanced distributed plasticity nonlinear fibre-beam column model using OpenSees (Spacone et al. 1996a,b and OpenSees 2013). A novel uniaxial material model developed by Kashani et al. (2015a) is used to simulate the inelastic buckling and low-cycle fatigue degradation of vertical reinforcing bars in bridge piers under cyclic loading. The finite element model is validated against the experimental data of RC bridge piers conducted by Lehman and Moehle (2000). The fibre element modelling technique that is used in this research was developed by Kashani et al. (2016), which employs the uniaxial material model developed in Kashani et al. (2015a). This bridge pier model is a generic distributed plasticity nonlinear fibre beam-column element which is capable of predicting multiple failure modes (confined concrete crushing, inelastic buckling and/or tension failure of longitudinal reinforcing bars, low-cycle fatigue) of RC components simultaneously. Therefore, it can accurately account for the impact of ground-motion characteristics on the nonlinear dynamic response of RC components. It should be noted that second order effects (P-Δ) are also included in the proposed fibre model using the Co-rotational formulation available in OpenSees (Neuenhofer and Filippou 1998).

Finally, using the spectrally matched and unmatched ground motions, a series of Incremental Dynamic Analyses (IDAs) are conducted on three prototype circular RC bridge pries of different heights taken from Lehman and Moehle (2000) test units. The selected bridge pier prototypes represent various elastic fundamental periods, T_1. A comparison is made between the nonlinear dynamic response of the proposed bridge piers obtained with the advanced model accounting for inelastic buckling and low-cycle fatigue of reinforcement and the conventional model without consideration of bar buckling and degradation. The parameters investigated include the low-cycle fatigue failure, the ground-motion types (FF, NFWP and NFPL), matching effect, and pulse effect (non-stationary content).

2. The proposed bridge pier models

Three bridge piers of different heights are employed in this study. The details of the proposed bridge piers are shown in Table 1. These columns are taken from the experimental test units reported in Lehman and Moehle (2000). The same ID as used in the experiment is employed here to identify these columns. The test specimens used in this study are units 415, 815 and 1015. A schematic illustration of these columns is shown in Fig. 1 and their corresponding dimensions and reinforcement details are summarised in the Table 1. In the Table 1, L/D is the ratio between column length (L) and column diameter (D), ρ_l is the longitudinal reinforcement ratio defined as a function of the total cross section area of the RC column, ρ_h is the volumetric ratio of the transverse reinforcement, $P/(A_g f_c)$ is the axial force ratio where P is axial force, A_g is the gross area of column cross section, and f_c is the concrete compressive strength. Further detailed information about the experimental tests and material properties is available in Lehman and Moehle (2000). The digital force-displacement data of these experiments are available at the UW-PEER column database (Berry et al. 2004).

Table 1 Details of experimental test units as reported in Lehman and Moehle (2000)

Column ID	Length L [mm]	L/D	Vertical Bar Dia.[mm]	No. of Vertical Bars	Horz. Bar Dia. [mm]	Horz. Bar Spacing [mm]	$P/(A_g f_c)$	ρ_l	ρ_h
415	2438.4	4	16	22	6.5	32	0.07	1.49	0.01
815	4876.8	8	16	22	6.5	32	0.07	1.49	0.01
1015	6096	10	16	22	6.5	32	0.07	1.49	0.01

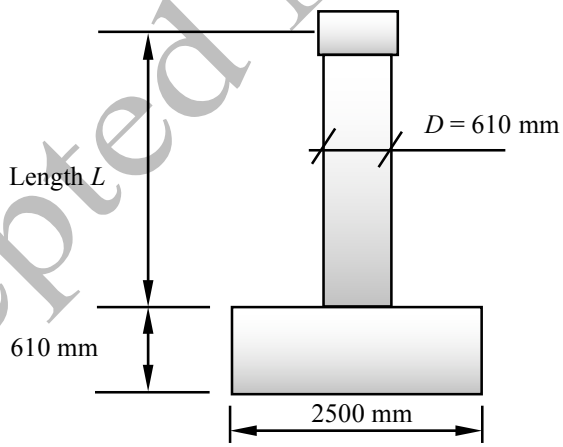

Fig. 1 Schematic view of the experimental units tested by Lehman and Moehle (2000)

2.1. Description of nonlinear fibre beam-column model

There are several methods available to model the nonlinear behaviour of RC structures. One of the most recent finite element techniques that is very popular among the earthquake engineering community is the fibre-based section discretisation technique (Spacone et al. 1996a,b). In this technique, the RC component is modelled using a beam-column element and the member cross section is discretised into a number of steel and concrete fibres at selected integration points. The material nonlinearity is represented through a uniaxial constitutive material model of steel (tension and compression) and concrete (confined core concrete and unconfined cover concrete). Therefore, the accuracy of the nonlinear model of RC components and structures is greatly influenced by the accuracy of the uniaxial material model. Accordingly, several researchers have developed material

models for concrete and reinforcing steel that can be used in nonlinear fibre beam-column element formulations. More recently, Kashani et al. (2015a) developed a new phenomenological uniaxial material model that has been implemented in OpenSees. Kashani et al. (2016) also developed an advanced fibre element modelling technique in OpenSees (OpenSees 2013) that employs their new uniaxial material model to simulate the nonlinear behaviour of circular RC bridge piers. This research employs the models in Kashani et al. (2015a) and Kashani et al. (2016) that have been extensively validated against a variety of experimental datasets. In this research the effect of geometric nonlinearity and large deformation is also considered in addition to the material nonlinearity. OpenSees employs Co-rotational formulation (Neuenhofer and Filippou 1998) to model the geometrical nonlinearity which is also used in this research.

2.2. Description of nonlinear uniaxial material models

2.2.1. Uniaxial material models for concrete

Concrete04 available in OpenSees is used to model the confined and unconfined concrete. The confined concrete material is located in the core of the RC column in which the concrete is confined by horizontal tie reinforcement. Unconfined concrete material represents the cover concrete. The *Concrete04* material model employs the Popovics curve (Popovics 1973) for the compression envelope and the Karsan-Jirsa model (Karsan and Jirsa 1969) to determine the slope of the curve for unloading and reloading in compression. For tensile loading, an exponential curve is used to define the envelope to the stress-strain curve. Further details are available in (Berry and Eberhard 2006). The parameters proposed by Mander et al. (1988) are used to model the effect of confinement on concrete in compression. The maximum compressive stress of the concrete and the strain at the maximum compressive strain (confined concrete strain at maximum stress) can be calculated using the equations developed in Mander et al. (1988). It should be noted that the maximum crushing strain of the confined concrete is limited by the fracture of the first horizontal tie/spiral reinforcement. In this research the empirical model developed by Scott et al. (1982) is used to define the confined concrete crushing strain in the confined concrete model.

2.2.2. Uniaxial material models for reinforcing steel

Two types of material models have been considered in the analyses. The first model is the conventional Giuffre-Menegotto-Pinto (GMP) model (1973). This model was modified by Filippou (1983) and later implemented in OpenSees as Steel02. The Steel02 accounts for the Bauschinger effect (Bauschinger 1887), but does not account for cyclic strength and stiffness degradation due to bar buckling and fatigue. The second model is the phenomenological uniaxial model developed by Kashani et al. (2015a). This model uses the generic Hysteretic material model available in OpenSees for its implementation. The generic Fatigue wrapper developed by Uriz (2005) is then wrapped to the Hysteretic material model to simulate the low-cycle fatigue failure of vertical reinforcing bars. Therefore, this combined model accounts for the influence of inelastic buckling and low-cycle fatigue degradation. Through a comprehensive parametric study the 'optimum' pinching parameters of the model under cyclic loading are obtained (Kashani et al. 2016). A more detailed discussion of the model development and calibration can be found elsewhere (Kashani et al. 2014, Kashani et al. 2016).

2.3. Finite element model validation against experimental test data

Fig. 2 shows the qualitative comparison of OpenSees simulation and the observed experimental results. Fig. 2 shows that the simulation results using *Steel02* material model can predict the nonlinear cyclic response accurately up to the maximum strength. However, as the lateral deformation of columns increases, severe strength degradation is observed in the experiment that cannot be simulated by *Steel02*. The simulation results using the buckling and fatigue model show that the failure mode of these columns is initiated by inelastic buckling of vertical bars. As the damage progresses after buckling of vertical bars the core concrete starts crushing. This is followed by fracture of vertical bars in tension due to low-cycle high amplitude fatigue. The simulation results are in good agreement with the experimental failure modes reported in Lehman and Moehle (2000). It is evident from Fig. 2 that

the proposed nonlinear fibre beam-column model is able to reliably simulate the nonlinear response of these bridge piers up to complete collapse.

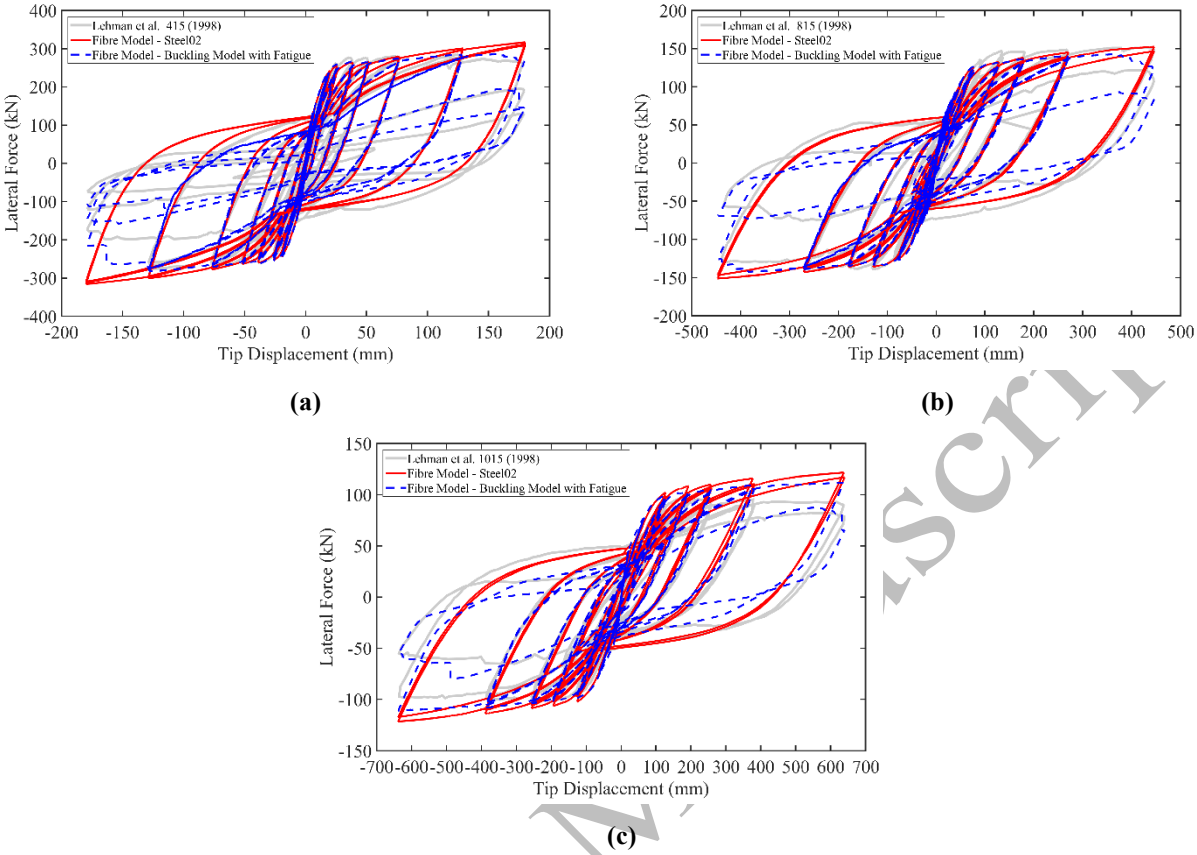

Fig. 2 Comparison of the computed response using OpenSees and observed experimental response: (a) test unit 415 (b) test unit 815 and (c) test unit 1015

3. Ground motion selection and matching

In this study three types of ground motions were considered. This includes Far-Field (FF), Near-Field without Pulse (NFWP) and Near-Field Pulse-Like (NFPL) record sets. Ground motions close to a ruptured fault can be significantly different than those further away from the seismic source. The near-field zone is typically assumed to be within a distance of up to 20km from a ruptured fault (PEER 2001, Baker 2007). Structures with medium to short natural vibration period are more vulnerable to near-field type ground motions (PEER 2001).

3.1. Ground-motion selection

FEMA P695 (2009) provides a list of ground motions of different types i.e. FF, NFPL and NFWP. The recorded acceleration series of these ground motions are available in the PEER-NGA West database (Ancheta et al. 2013) which is employed in this research. The FEMA P695 document recommends a set of 22 FF records with an average moment magnitude of M_w=7.0. Each record has two horizontal and one vertical component. Besides, FEMA P695 also recommends a total of 28 NFPL and NFWP ground-motion records with 56 components that are all available in the PEER-NGA West database. 14 of these ground motions are NFPL and 14 records are NFWP. These ground motions have an average magnitude of M_w=7.0 and are taken from 14 events that happened from 1976 to 2002. 7 of these ground motions are recoded in the United States and 5 others come from other countries around the world. 11 ground-motion stations were located in stiff soil sites, 15 of them in very stiff soil sites and the rest correspond to rock sites. Values of their PGAs vary from 0.22 g to 1.43 g with a mean value of 0.6 g. The PGVs of these ground motions vary between 0.30 m/s and

0.167 m/s with a mean value of 0.84 m/s. The elastic response spectra of all ground motions as well as the mean response spectrum of each group are shown in Fig. 3.

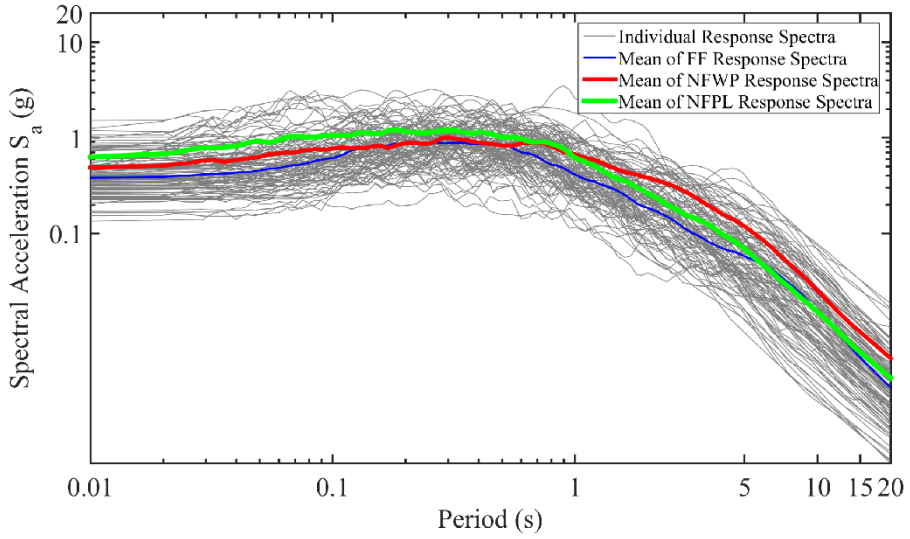

Fig. 3 Elastic response spectra of FEMA P695 recommended ground motions

3.2. Matching selected ground motions to the target response spectra

In order to determine the effects of the non-stationary characteristics of the acceleration time series (i.e. envelope and pulse timing) the influence of the spectral content (estimated stationary content) is removed herein by spectrally matching all records to a common response spectrum. Thus, we ask whether there is any statistical difference between the response of our bridge piers to near/far field and pulse/non-pulse like records when the influence of the spectral differences (stationary content) is removed. To this end, the Reweighted Volterra Series Algorithm (RVSA) proposed by Alexander et al. (2014) is employed. This spectral matching process keeps the non-stationary characteristics (i.e. the general envelope and timing of main pulses) of the seed record largely unchanged but it matches the target response spectrum. Further details of this procedure are available in Alexander et al.

5 records are selected from each of the ground-motion sets recommended in FEMA P695 and are tabulated in Table 2. The records are taken from the PEER-NGA West database. Thus, these three ground motion groups are mapped into nine cases, each of which may have different stationary and non-stationary content. A full list of cases is presented in Table 3. The matched response spectra of each case are shown in Fig. 4. And an example of the original and matched ground motion is shown in Fig. 5.

Table 2 Selected ground motions from PEER-NGA West database

ID	Record Set	Record File Name	PGA (g)	PGV (cm/s)
FF1	Far Field	FRIULI.A_A-TMZ270.AT2	0.32	30.52
FF2	Far Field	IMPVALL.H_H-DLT352.AT2	0.35	33.00
FF3	Far Field	SUPER.B_B-ICC000.AT2	0.36	48.07
FF4	Far Field	SUPER.B_B-POE270.AT2	0.47	41.17
FF5	Far Field	MANJIL_ABBAR--T.AT2	0.50	50.59
NFWP1	Near Field without Pulse	GAZLI_GAZ090.AT2	0.86	67.65
NFWP2	Near Field without Pulse	IMPVALL.H_H-CHI282.AT2	0.25	29.90
NFWP3	Near Field without Pulse	LOMAP_BRN000.AT2	0.46	51.39
NFWP4	Near Field without Pulse	NORTHR_STC180.AT2	0.46	60.14
NFWP5	Near Field without Pulse	DENALI_PS10-317.AT2	0.30	65.96
NFPL1	Near Field Pulse Like	IMPVALL.H_H-E07230.AT2	0.47	113.14
NFPL2	Near Field Pulse Like	SUPER.B_B-PTS225.AT2	0.43	134.29
NFPL3	Near Field Pulse Like	CAPEMEND_PET090.AT2	0.66	88.51
NFPL4	Near Field Pulse Like	CHICHI_TCU065-E.AT2	0.79	125.35
NFPL5	Near Field Pulse Like	CHICHI_TCU102-N.AT2	0.17	66.43

Table 3 Matrix of artificial records with different stationary and non-stationary content

		Non-stationary content		
		a (FF)	**b (NFWP)**	**c (NFPL)**
Stationary Content	**Case I (FF)**	FF set matched to mean of FF	NFWP set matched to mean of FF	NFPL set matched to mean of FF
	Case II (NFWP)	FF set matched to mean of NFWP	NFWP set matched to mean of NFWP	NFPL set matched to mean of NFWP
	Case III (NFPL)	FF set matched to mean of NFPL	NFWP set matched to mean of NFPL	NFPL set matched to mean of NFPL

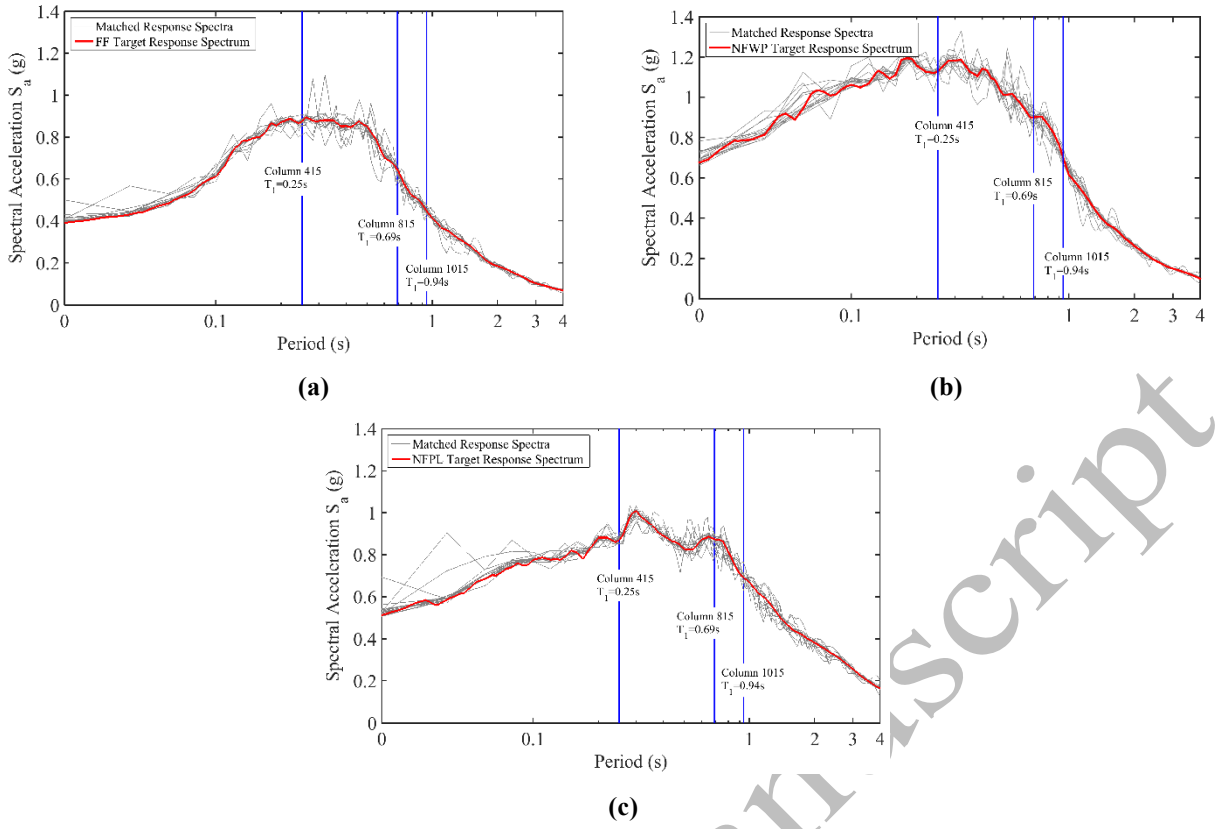

Fig. 4 Matched response spectra of selected ground motions: (a) Case I, (b) Case II and (c) Case III

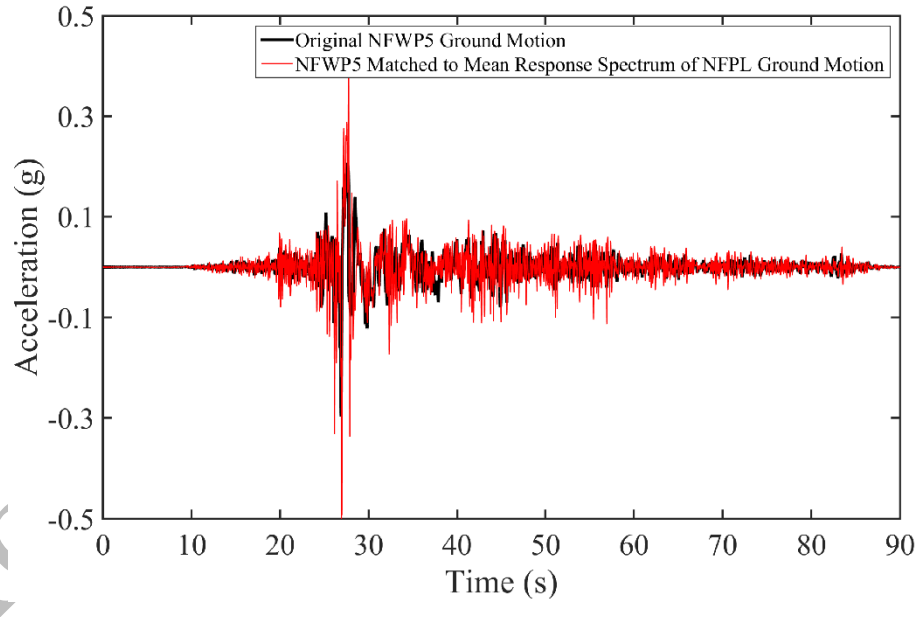

Fig. 5 Example of an original and matched ground-motion history of acceleration

4. Incremental dynamic analysis (IDA), results and discussion

In this research, a series of IDAs (Vamvatsikos and Cornell 2002). are performed, in order to explore the influence of material degradation (buckling and fatigue) on the nonlinear dynamic response of RC bridge piers. The IDAs are conducted for each group of matched and equivalent unmatched ground motions that were discussed in section 3 of this paper. The intensity of ground motion was characterised herein by the value of its spectral acceleration (Sa) at the fundamental period (T_1) of the structures i.e. Sa(T_1).

The distribution of peak drifts (mean and standard deviation) is estimated from the structural responses. To this end, a log-normal distribution was fitted by the method of moments (Baker, 2015).

4.1. Definition of ultimate limit state drift of proposed columns

In order to compare the results of different modelling techniques the collapse load should be defied precisely. Fig. 6 shows nonlinear pushover response of all three columns. The failure point of each column is defined as the minimum of either bar buckling/concrete crushing in compression or fracture of first bar in tension. These points are identified by reading the material responses at the first critical fibre section. The results show that the failure of columns 415 at 815 is governed by bar buckling and concrete crushing at about 6% and 7% respectively. However, the failure of column 1015 is governed by the fracture of bars in tension at about 11% drift. In the following sections, the comparison of IDA results between the two models is at the failure drifts that are identified here.

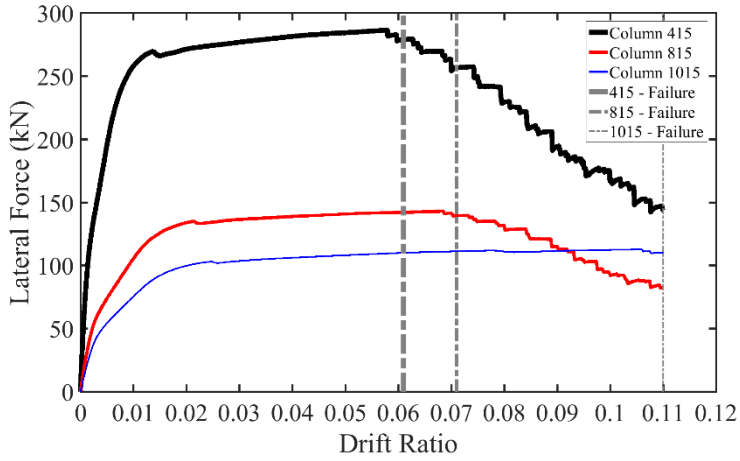

Fig. 6 Example of an original and matched ground-motion history of acceleration

4.2. Influence of material degradation on nonlinear response

Fig. 7 shows the analyses results of the Case I ground motions. In Case I, all of the ground motions are matched to the mean response spectrum of the FF ground motions. Fig. 7(a) shows that column 415, which includes the effect of buckling and fatigue, would fail at smaller drift (at about 7% drift) than that of the model without buckling and fatigue. The column 815 (Fig. 7(b)) also shows similar behaviour to 415. However, Fig. 7(c) shows that the response of the column 1015 using the model including buckling and fatigue and the model without buckling and fatigue are almost identical. This indicates that material degradation due to buckling and fatigue would not have a significant effect in the behaviour of Model 1015.

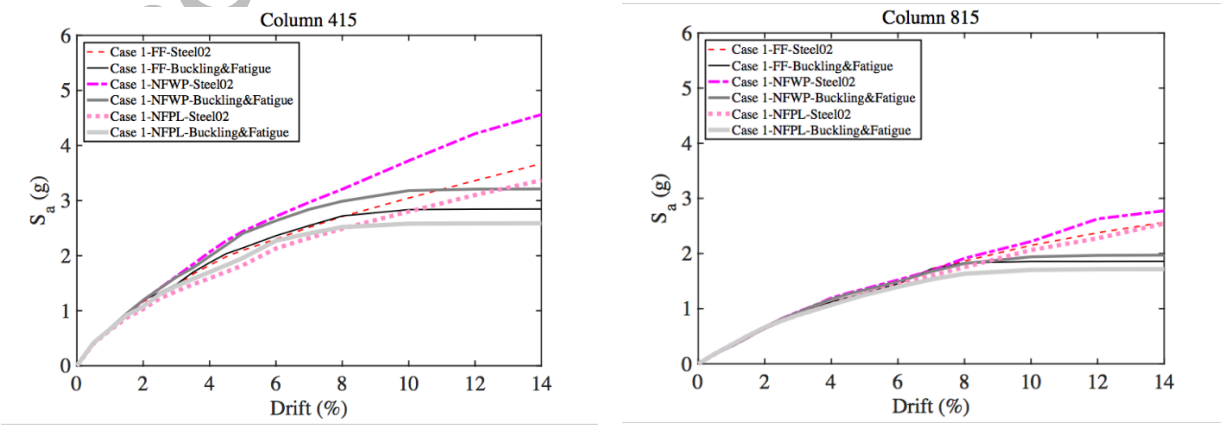

(a) **(b)**

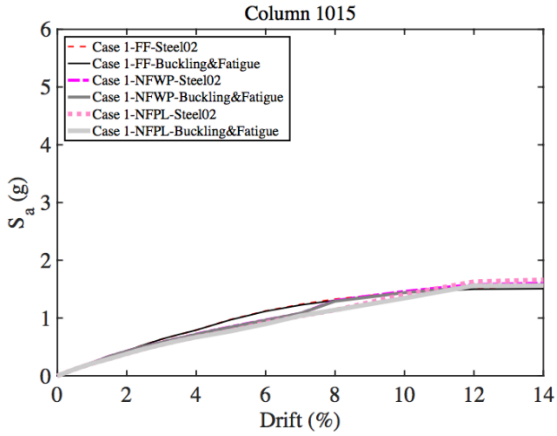

(c)

Fig. 7 Mean response of the RC columns under Case I ground motions: (a) Column 415, (b) Column 815 and (c) Column 1015

A comparison of Figs. 7(a), (b) and (c), shows that the effect of buckling and fatigue on the nonlinear dynamic response of the structure become less significant as the pier height (slenderness) increases from model 415 to model 1015. The impact of considering buckling and fatigue in strength loss and collapse capacity of each column is shown in Fig 8. The ratios of the mean computed responses (ratios of mean S_a) of the model including buckling and fatigue and the model without buckling and fatigue, for each column, under Case I ground motions are plotted in Fig. 8. The Fig. 8 shows that the significant strength loss in columns 415 and 815 starts at about 6% drift ratio, where severe buckling occurs. However, the ratio of the mean response of both models for column 1015 is almost 1, which indicates cyclic degradation does not have any significant influence on the nonlinear dynamic response of this column.

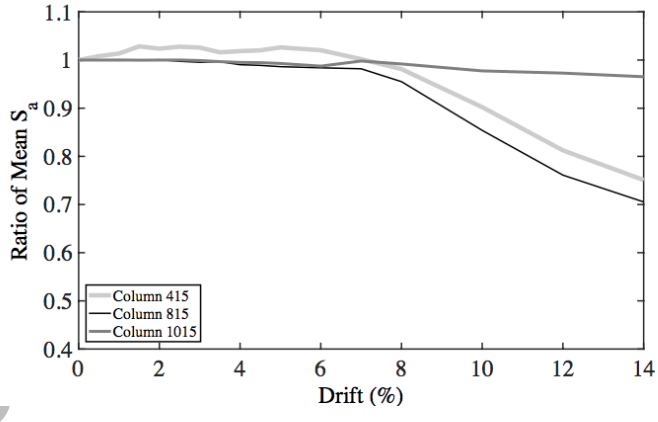

Fig. 8 Ratio of mean response (mean S_a) of the model including buckling and fatigue to the model without buckling and fatigue (Case I)

Fig. 9 shows the results from analyses for Case II ground motions. In Case II, all of the ground motions are matched to the mean response spectrum of the NFWP ground motions. The comparison of the results in Fig. 9 and Fig. 7 shows that there is a similar trend in strength loss and collapse capacity of the columns. The only visible difference between Fig. 9 and Fig. 7 is the variation between the computed responses of each model (e.g. comparing the model without buckling and fatigue effect with itself under different sets of ground motions). The results show that the variation between the results in columns 415 and 815 is smaller in Fig. 9. However, the variation between the results is larger in column 1015 in Fig. 8 compared to Fig. 7. Overall the results show that considering buckling and fatigue has a more severe effect on strength loss and collapse capacity of the columns in Case II relative to Case I.

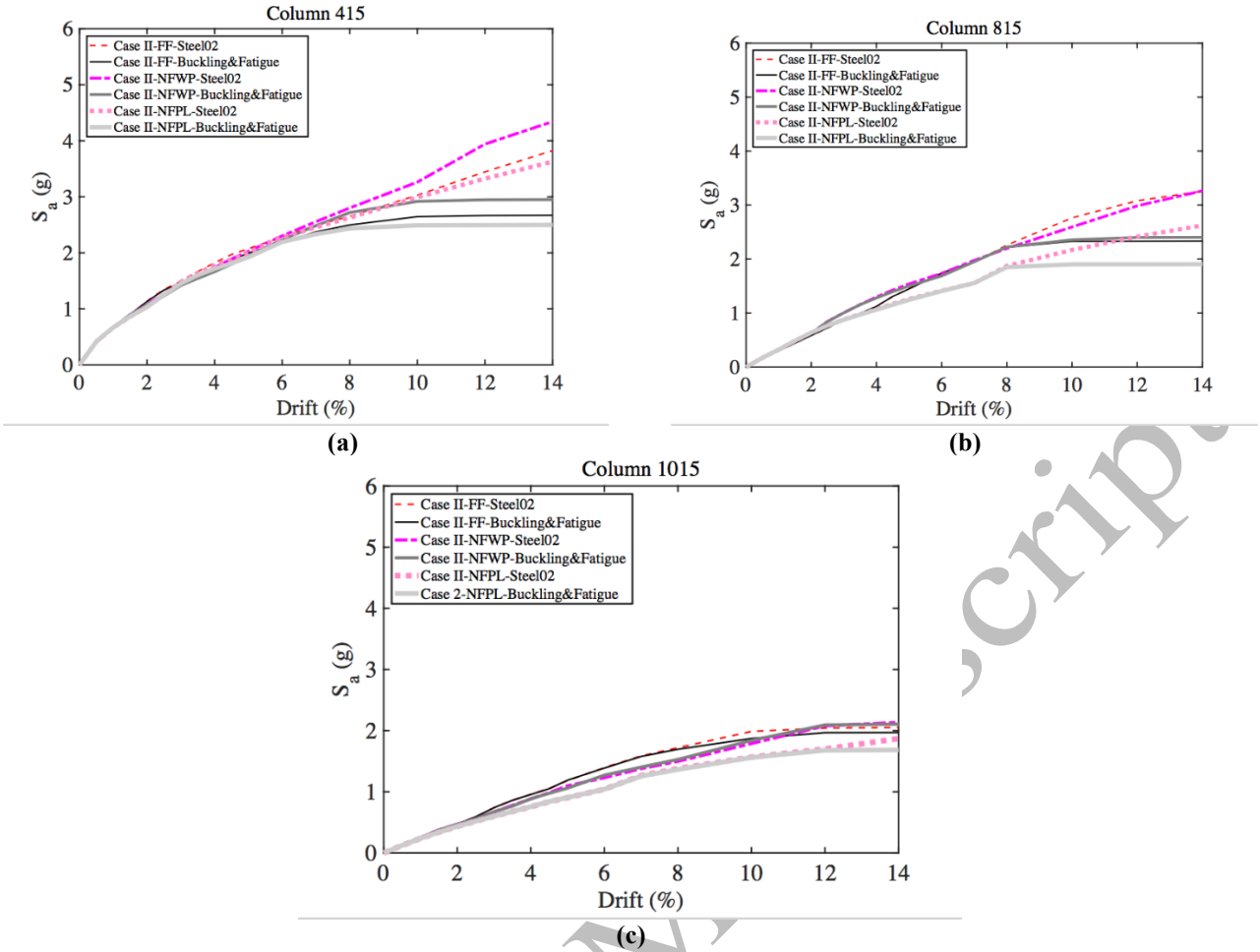

Fig. 9 Mean response of the RC columns under Case II ground motions: (a) Column 415, (b) Column 815 and (c) Column 1015

The ratio of the mean computed responses of the model including buckling and fatigue and the model without buckling and fatigue, for each column, under Case II ground motions are plotted in Fig. 9. Fig. 9 clearly shows that buckling and fatigue have a more severe effect on capacity reduction in all columns in Case II relative to Case I. However, the effect of buckling and fatigue on response of column 1015 is still much less than for columns 415 and 815. The Fig. 10 shows that the significant strength loss in columns 415 starts at about 4% drift ratio, which is slightly smaller than Case I. In contrast the severe strength loss of column 815 starts at about 8% drift ratio which slightly larger than Case I. However, the ratio of the mean response of both models for column 1015 is almost 1, which is very similar to computed response in Case I.

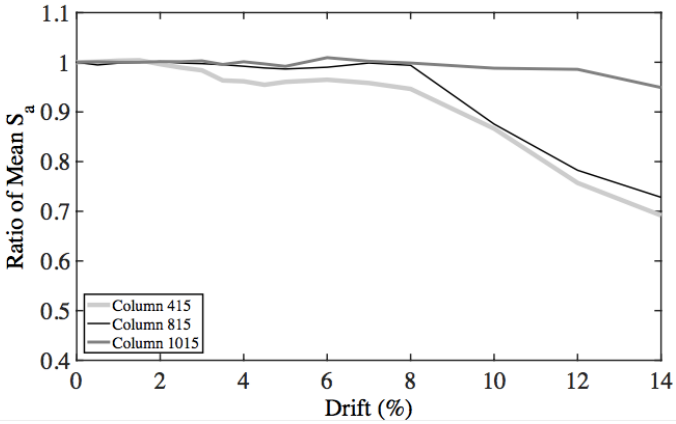

Fig. 10 Ratio of mean response (mean S_a) of the model including buckling and fatigue to the model without buckling and fatigue (Case II)

Fig. 11 shows the analyses results of the Case III ground motions. In Case III, all of the ground motions are matched to the mean response spectrum of the NFPL ground motions. It is clear from Fig. 11 that overall the computed responses of columns 415 and 815 in Case III are much lower than the computed responses in Case I and Case II. However, this is not significant for column 1015. Despite the significant reduction in the Sa in columns 415 and 815, there is still a severe strength loss in the model including buckling and fatigue. The reduction in collapse capacity in column 415 is higher than Case I but it is lower than Case II. It was also observed that reduction in collapse capacity of column 815 in the model including buckling and fatigue is higher than Case I and Case II. However, the strength loss is much lower in column 1015 in Case III compare to Cases I and II.

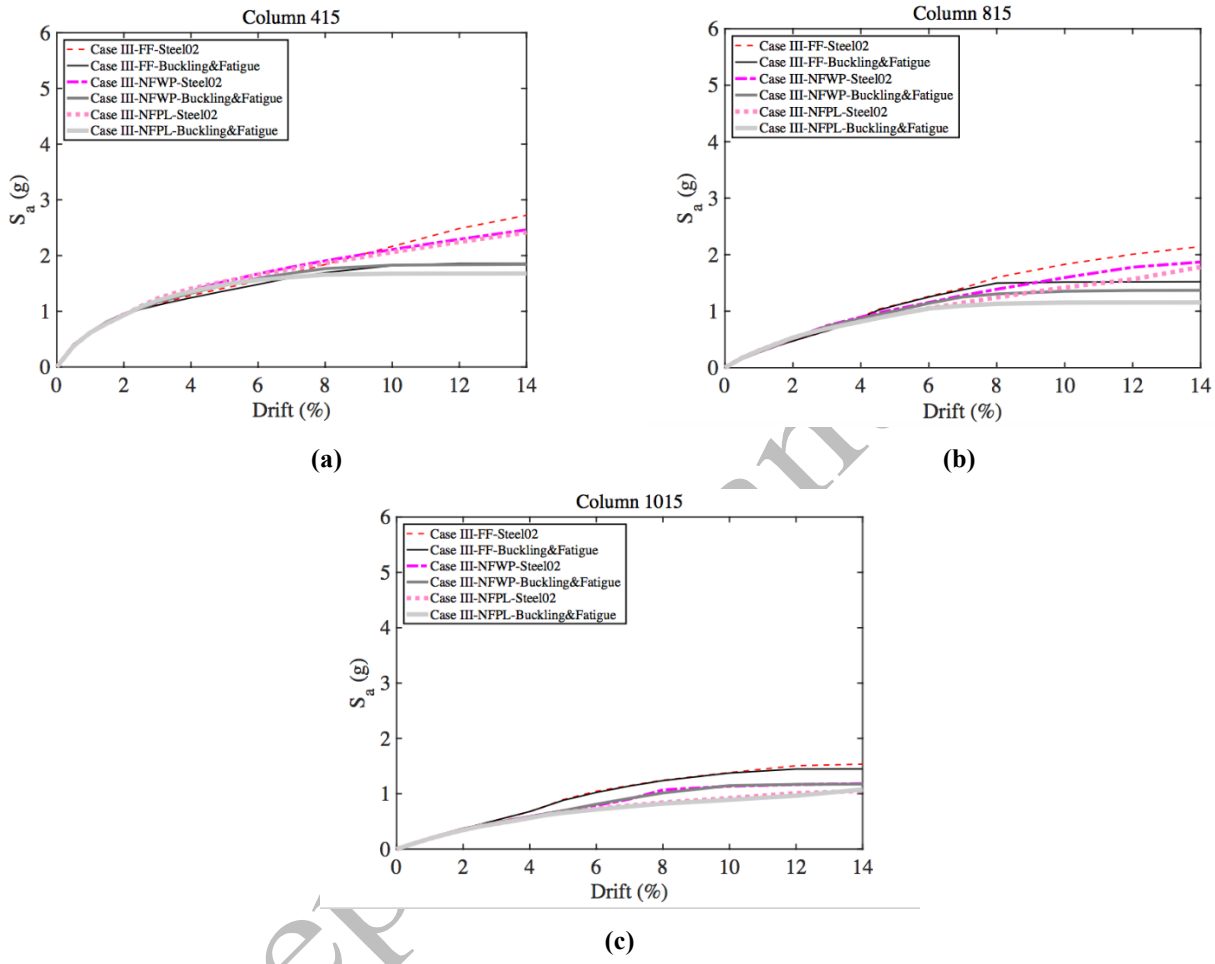

Fig. 11 Mean response of the RC columns under Case III ground motions: (a) Column 415, (b) Column 815 and (c) Column 1015

The ratios of the mean computed responses of the model including buckling and fatigue and the model without buckling and fatigue, for each column, under Case III ground motions are plotted in Fig. 12. Fig. 12 shows that the capacity reduction in columns 415 and 815 due to buckling and fatigue is similar to Case I and Case II. It also shows that in Case III, similar to Case I and Case II, buckling and fatigue does not have a significant impact on the response of column 1015. The Fig. 12 shows that the significant strength loss in columns 415 and 815 starts at about 6% drift ratio, which is very similar to Case 1 (Fig. 8). The ratio of the mean response of both models for column 1015 is almost 1, which is very similar to Case I and II (Fig. 8 and Fig. 10)

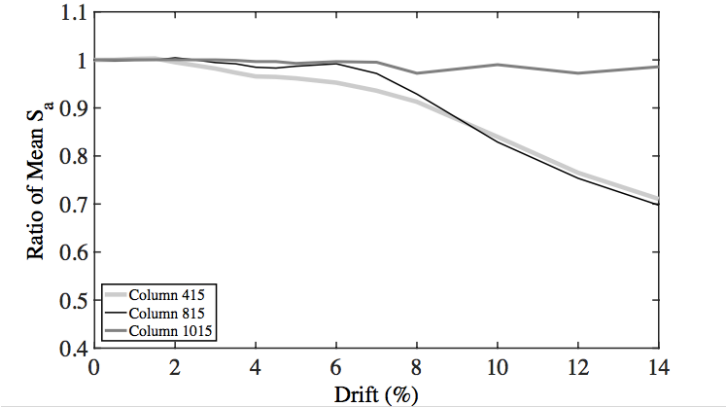

Fig. 12 Ratio of mean response (mean S_a) of the model including buckling and fatigue to the model without buckling and fatigue (Case III)

To conclude this section, it can be seen that two main effects have been observed. The first observation, as expected, is the frequency dependency of the response. For example, the maximum computed responses (Sa) of the columns 415 and 815 are much higher in Case I and Case II compared to Case III whereas the computed maximum responses of column 1015 was almost identical for the three ground-motion cases here studied (Case I,II and III). This phenomenon is due to the nature of ground motions that is discussed in detail in section 4 of this paper. The second observation is the trend between the impact of material degradation and the shear span to depth ratio of the column (L/D). A comparison of the nonlinear cyclic and pushover responses of column 1015 with that of columns 415 and 815 in Fig. 2 and Fig. 6 shows that as the column height increases the buckling effect is less visible in the cyclic loops of these columns. For example, the failure mode of column 415 starts with buckling followed by core concrete crushing at about 6% drift (Fig. 6) and subsequently fracture of the bars in tension due to low-cycle fatigue degradation at about 6% drift under repeated cycles (Fig. 2). Column 815 also shows similar behaviour. However, the failure mode of the column 1015 is different from that of columns 415 and 815. The failure mode in column 1015 starts with buckling (not as severe as columns 415 and 815) but is followed by fracture of bars in tension without any severe core concrete crushing. This behaviour was observed in the experimental testing by Lehman and Moehle (2000) and numerical modelling by Kashani et al. (2016) and also reported by other researchers (Berry and Eberhard 2003, 2006). Similar differences are appreciated in the nonlinear dynamic response of column 1015 in the IDA graphs. Therefore, it is evident that the proposed model that includes buckling and fatigue degradation, is capable of capturing multiple failure modes.

4.3. Influence of ground-motion matching

This section discusses the influence of the matching process on the nonlinear response of the structures with reference to NFPL ground motions. To this end, the responses of column 815 subjected to matched and unmatched records for Case III are compared. The model that includes the effects of buckling and fatigue is considered here. Fig. 12 shows the computed response of column 815 under matched (Fig. 13 (a)) and unmatched (Fig. 13 (b)) ground motions. Fig. 13 shows the mean and mean ± standard deviation of the computed response. The results presented in Fig. 13 correspond to the mean of fifteen ground motions (FF, NFWP and NFPL) matched to the mean of NFPL response spectrum. As expected, Fig. 13 shows that the computed response under matched ground motions has smaller dispersion than that of unmatched ground motion. The matching process helped to reduce the frequency-related record-to-record variability in the ground-motion set. It should be noted that Fig. 13 is only an example of comparison between response of structures subjected to matched and unmatched ground motions. Similar behaviour was observed in all other cases. Therefore, the effect that is being seen in the response is purely due the non-stationary components of the ground motions i.e. near-field and pulse effects versus far-filed ground motions. However, it should be noted that this process is only adequate for comparison of the mean responses of each group of ground motions. To

identify other effects and dispersion of ground motions further analyses are required which are out of the scope of this paper.

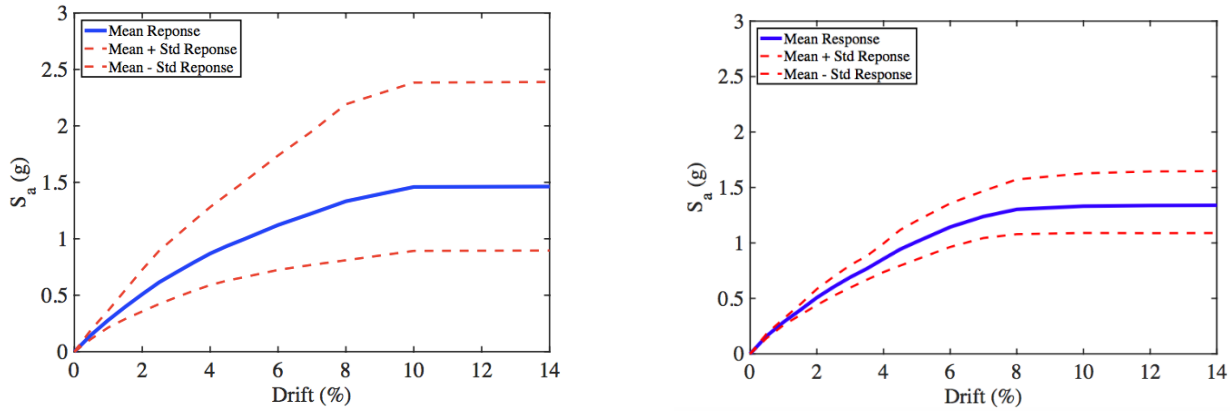

(a) **(b)**

Fig. 13 Matching effect on mean response of column 815 under Case III ground motions: (a) unmatched ground motions and (b) matched ground motions

4.4. Influence of ground-motion type and target spectrum on nonlinear response

In order to quantify the influence of ground motion patterns on the nonlinear response, the computed responses for each case are normalised to the response for the target ground motion. Please note that in this section all of the computed responses presented were obtained with the model including buckling and fatigue. For example, Fig. 14(a-c) shows the normalised mean capacity ($S_a(T_1)$) at different drift levels for columns 415, 815 and 1015 for Case I ground motions. In this case the response of columns subjected to NFWP and NFPL ground motions are normalised to the response of columns subjected to spectrally matched FF ground motions. The normalised response of columns subjected to FF ground motions are not shown in Fig. 14 as it will be 1 for all drift ratios. It should be noted that if the system was linear all of the graphs in Fig. 14 would be 1.0 for all drift ratios. This is because all of the ground motions have elastic response spectra that have been matched to the mean response spectrum of the FF ground motions. The differences shown in Fig. 14 are due to the impact of material nonlinearity and its interaction with the ground-motion type (i.e. FF, NFWP and NFPL). Figs. 14(a) and (b) show that the response of the columns 415 and 815 subjected to NFWP ground motions is about 15% and 8% higher than the spectrally matched FF ground motions. However, the response of columns 415 and 815 subjected to NFPL ground motions is about 15% smaller than the spectrally matched FF ground motions. This clearly shows the near field and pulse effects on the structures. In contrast, Fig. 14(c) shows that the response of column 1015 under NFWP and NFPL ground motions is about 15% and 20% smaller, respectively, in comparison with the spectrally matched FF ground motions.

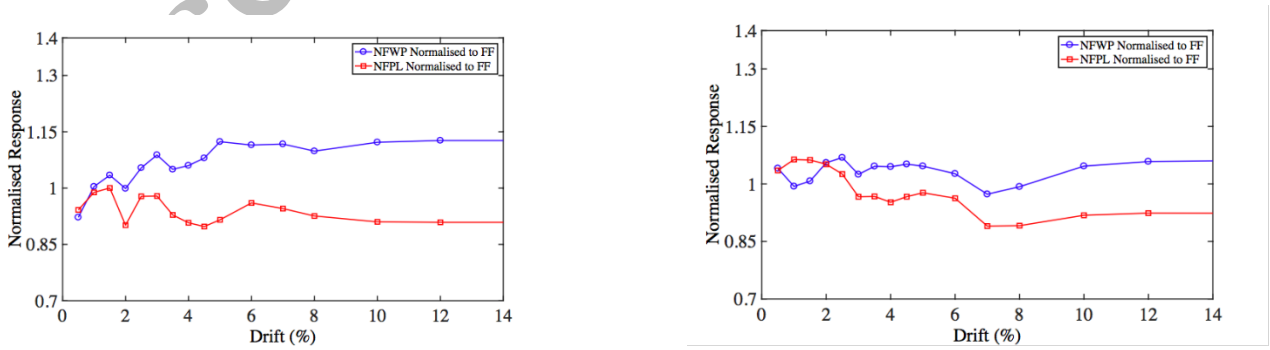

(a) **(b)**

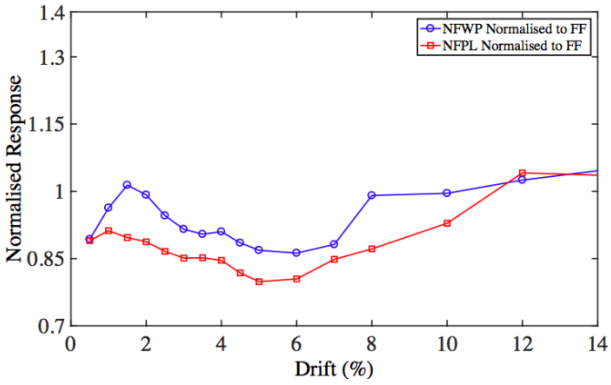

(c)

Fig. 14 Normalised mean acceleration response of Case I ground motions: (a) Column 415, (b) Column 815 and (c) Column 1015

Fig. 15(a-c) shows the normalised response of columns 415, 815 and 1015 for Case II ground motions. In Fig. 15, the response of all columns subjected to FF and NFPL ground motions are normalised to the response of columns subjected to spectrally matched NFWP ground motions. Fig. 15 shows the near field effect on the response of columns. Fig.15 shows that as the elastic period of the structure increases (the height of column increases) the near field effect (on the response of columns under FF ground motions) increases. However, it also shows that the mean capacity response of columns subjected to NFPL ground motion reduces which is due to the type of the ground motion (pulse-like ground motion).

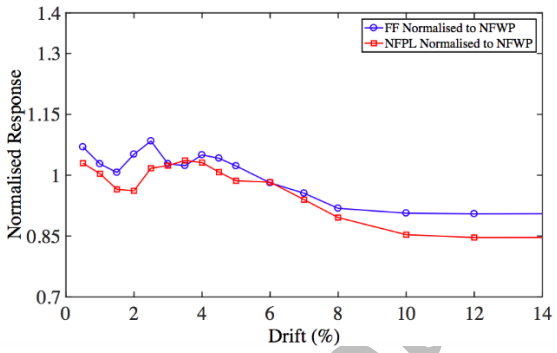

(a)

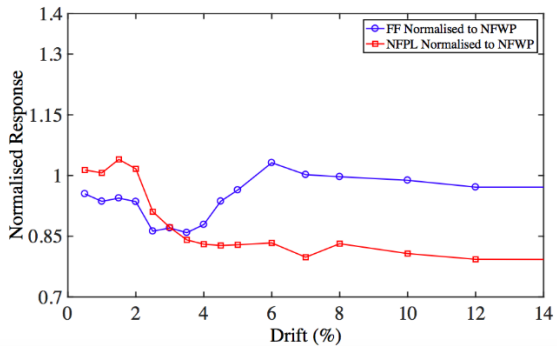

(b)

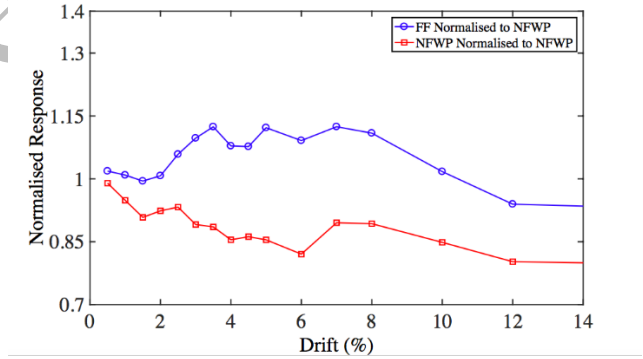

(c)

Fig. 15 Normalised mean acceleration response of Case II ground motions: (a) Column 415, (b) Column 815 and (c) Column 1015

Fig. 16(a-c) shows the normalised response of columns 415, 815 and 1015 for Case III ground motions. In Fig. 16, the response of all columns subjected to FF and NFWP ground motions are normalised to the response of columns subjected to spectrally matched NFPL ground motions. Fig.

16 clearly shows the pulse effect on the response of the structures. It shows that by increasing the period of the structure the pulse effect also increases. This is a very important finding as the proposed model in this paper can accurately capture this phenomenon. Fig. 16(a) shows that the pulse effect on the response of column 415 which has the lowest period is not significant. However, as the drift of structure increases the response increases by about 10% for both FF and NFWP ground motions. Fig. 16(b) shows similar behaviour, however, given the elastic period of column 815 is longer than column 415 the pulse effect is more significant. Finally, Fig. 16(c) shows that the pulse effect can increase the response of the column by about 50%. One of the reasons is that the column 1015 has a larger elastic period compared to columns 415 and 815. The other reason for this is due to the much higher energy of the FF ground motion matched to NFPL which has the long duration of FF since very little temporal variation is introduced by the RVSA matching procedure (Alexander et al., 2014) plus the pulse-like nature of NFPL ground motion. This is a very important finding and is an area for future research.

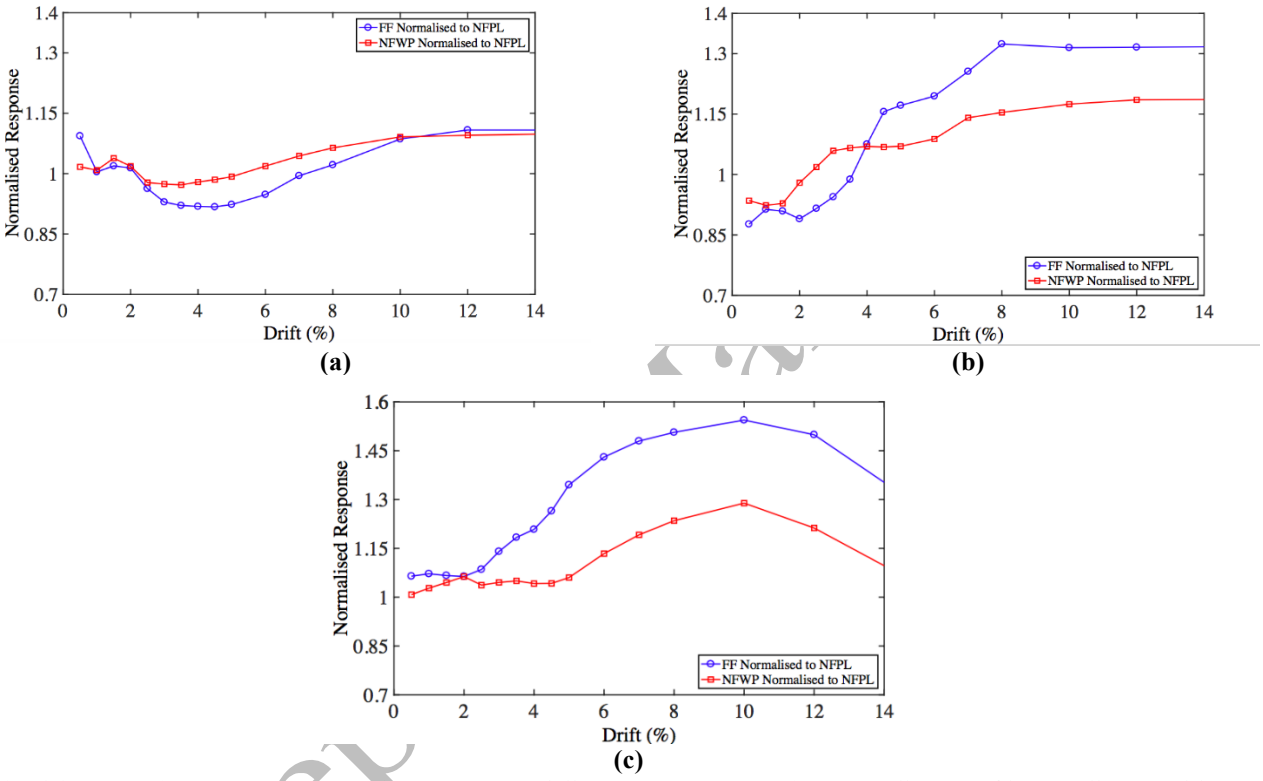

Fig. 16 Normalised mean acceleration response of Case III ground motions: (a) Column 415, (b) Column 815 and (c) Column 1015

The IDA results and comparison with the monotonic and cyclic static analyses clearly confirm that the onset of bar buckling depends on the load history history. This can be simply explained by behaviour of a single bar with a known buckling length, subject to a simple cyclic load history. If we push the bar to compression, it yields at about the yield strain of steel, and then buckles. Following buckling, depends how far the bar is pushed in post-buckling region the response in the next cycle will be different. Now, if we change the loading protocol and pull the bar in tension to yield, and then push it to compression, it will buckle earlier depends on the tension strain. Kashani et al. (2015a) developed a simple model to account for the effect of tension strain on the onset of buckling of bars. Furthermore, when bars buckle, they fracture much quicker under repeated cyclic loading. This is because inelastic buckling reduces the low-cycle fatigue life of reinforcing bars (Kashani et al. 2015b). Furthermore, all of the proposed columns were design according to Caltrans standard (Caltrans 2013). However, severe buckling was observed in all of the experiments. This is because the interaction between the horizontal tie reinforcement and vertical bars is not considered in the current seismic design codes. Therefore, depends on the stiffness of horizontal tie reinforcement and loading history, the inelastic buckling of vertical bars may or may not happen within the limit of

seismic design action. If vertical bars buckle within the limit of seismic design action, bars will quickly fracture in tension due to low-cycle fatigue, which is not a favourable failure mode. This is a very complicated issue, and despite the significant effort by various researchers, it is still an open issue, which should be addressed in the future research.

5. Conclusions

A series of IDAs are conducted on three prototype RC bridge piers with various heights. The acceleration records were selected from the ground motions suggested in FEMA P695. Three types of ground motions such as FF, NFWP and NFPL are considered. To investigate the impact of the non-stationary components associated with different ground-motion types (e.g. near-field and pulse effect compared to far field effect) and exclude it from other ground-motion frequency-related characteristics, a response spectrum matching technique is employed. Three analysis cases are considered. In Case I all ground motions are matched to the mean response spectrum of FF ground motions, in Case II all ground motions are matched to the mean response spectrum of NFWP ground motions and in Case III all ground motions are matched to the mean response spectrum of NFPL ground motions. The main conclusions of this study are summarised as follows:

1. It was found that considering inelastic buckling and low-cycle fatigue results in severe strength loss in columns 415 ($L/D = 4$) and 815 ($L/D = 8$). However, it did not have a significant influence on the response of column 1015 ($L/D = 10$).

2. The influence of inelastic buckling and degradation on the response of the columns is reduced by increasing the height of the columns. Similar behaviour is observed in static cyclic testing of these columns. This is because when the column's height increases, the base plastic rotation reduces for a given tip displacement. Therefore, the plastic deformation capacity increases. As a result the failure mode is generally governed by fracture of the vertical reinforcement in tension. In other words, the taller the column the more likely it fails in tension before it experiences any significant cyclic degradation due to inelastic buckling and low-cycle high-amplitude fatigue. This is also in good agreement with large-scale shake table results report by Brown and Saiidi (2011).

3. It was found that the pulse effect can amplify the peak response by about 50%. However, this is different at different drift ratios. It is shown that as the structure starts behaving nonlinearly the period changes and as a result the pulse effect may change.

4. It was found that the peak response of columns 415 and 815 reduced in Case III compared to cases I and II. However, the peak response of column 1015 remained unchanged in Case III. This suggests that the structures with longer periods are more vulnerable to NFPL ground motions. This is in contrast with past results (PEER 2001), and is an area for further investigation in the future research.

5. The structures analysed in this paper were designed according to modern seismic design code (Lehman and Moehle 2000). However, severe buckling was observed in both experiment and numerical modelling. This is mainly because the seismic design codes (e.g. Caltrans) have requirements for confining reinforcement and maximum tie spacing, but these requirements do not fully restrain vertical bars against buckling. The main factor affecting the buckling of bars inside concrete is the ratio of flexural rigidity of vertical bars to stiffness of tie reinforcement, which is in good agreement with Dhakal and Maekawa (2002). This is still and open issue and is an area for future research.

6. The outcome of this study shows that the material degradation due to inelastic buckling and low-cycle fatigue of reinforcement still affects the nonlinear dynamic response. Therefore, these parameters should be considered in seismic performance, design, analysis and assessment of

existing and new structures. The response spectrum analysis and/or capacity spectrum techniques that rely on the elastic period and static inelastic response (pushover curves) of structures are not accurate enough for performance prediction. They can be used as a simplified starting point; however, more comprehensive analyses are required depending on the complexity and importance of the structure, ground-motion characteristics and construction materials of the structure.

7. The method proposed and used in this paper provides a platform for the earthquake engineering community (researchers and practitioners) to use in future research. The nonlinear structural model is readily available in OpenSees and the response spectrum matching software is available for free download at https://sites.google.com/site/volterramatch/.

References

Alexander NA, Chanerley AA, Crewe AJ, Bhattacharya S. 2014. "Obtaining spectrum matching time series using a reweighted volterra series algorithm (RVSA)." *Bulletin of the Seismological Society of America* 104 (4): 1663-1673.

Ancheta TD, Darragh RB, Stewart JP, Seyhan E, Silva WJ, Chiou BSJ, Wooddell KE, Graves RW, Kottke AR, Boore DM, Kishida T, Donahue JL. 2013. *PEER NGA-West2 Database.* Berkeley: Pacific Earthquake Engineering Research Center.

ASCE. 2010. *Minimum Design Loads for Buildings and Other Structures.* ASCE/SEI 7-10, Reston,: American Society of Civil Engineers.

Baker JW. 2015. "Efficient Analytical Fragility Function Fitting Using Dynamic Structural Analysis." *Earthquake Spectra* 31: 579-599.

Baker JW. 2007. "Quantitative classification of near-fault ground motions using wavelet analysis." *Bulletin of the Seismological Society of America* 97 (5): 1486-1501.

Bauschinger J. 1887. "Variations in the elastic limit of iron and steel." *The J. of the Iron and Steel Institute* 12 (1): 442-444.

Berry M, Eberhard MO. 2003. *Performance Models for Flexural Damage in Reinforced Concrete Columns.* Berkeley: Pacific Earthquake Engineering Research Centre.

Berry M, Parrish M, Eberhard M. 2004. *Performance Database User's Manual, PEER, Univ. of Calif. Berkeley.* Accessed 2013. www.ce.washington.edu/~peera1.

Berry MP, Eberhard MO . 2006. *Performance modeling strategies for modern reinforced concrete bridge columns.* Berkeley: Pacific Earthquake Engineering Research Centre.

Brown B, Saiid Saiidi M,. 2011. "Investigation of effect of near-fault motions on substandard bridge structures." *Earthquake Engineering and Engineering Vibration* 10 (1): 1–11.

Caltrans. 2013. "Seismic Design Criteria." *Caltrans* VERSION 1.7.

Chandramohan R, Baker JW, Deierlien GG. 2015. "Quantifying the influence of ground motion duration on structural collapse capacity using spectrally equivalent records." *Earthquake Spectra.* doi:http://dx.doi.org/10.1193/122813EQS298MR2.

Chang GA, and Mander JB. 1994. *Seismic energy based fatigue damage analysis of bridge columns: Part I – Evaluation of seismic capacity.* NCEER-94-0006.

Chatfield, Chris. 2003. *The Analysis of Time Series: An Introduction, Sixth Edition.* Chapman and Hall/CRC .

Cornell CA. 1997. "Does Duration Really Matter?" *FHWA/NCEER Workshop on the National Representation of Seismic Ground Motion for New and Existing Highway Facilities.* Burlingame,: National Center for Earthquake Engineering Research. 125-133.

Dhakal RP, Maekawa K. 2002. "Reinforcement stability and fracture of cover concrete in reinforced concrete members ." *Journal of Structural Engineering* 128 (10): 1253-1262.

Eurocode 8. 2010. "Design provisions for earthquake resistance of structures - Part 2: Bridges." *BS EN 1998-2:2005 +A1:2009.*

FEMA P695. 2009. *Quantification of Building Seismic Performance Factors.* Washington: Federal Emergency Management Agency.

FEMA. 2012. *Seismic Performance Assessment of Buildings, Volume 1 - Methodology.* Washington: Federal Emergency Management Agency.

Filippou FC, Popov EP, Bertero VV. 1983. *Effects of Bond Deterioration on Hysteretic Behavior of Reinforced Concrete Joints.* Berkeley: UCB/EERC, Univ. of Calif. Berkeley.

Hancock J, Bommer JJ. 2006. "A State-of-Knowledge Review of the Influence of Strong-Motion Duration on Structural Damage." *Earthquake Spectra* 22 (3): 827–845.

Hancock J, Bommer JJ. 2004. "The effective number of cycles of earthquake ground motion." *Ertq Eng Struct Dyn* 34: 637–664.

Hancock J, Bommer JJ. 2007. "Using spectral matched records to explore the influence of strong-motion duration on inelastic structural response." *Soil Dyn Eartq Eng* 27: 291–299.

Ibarra LF, Medina RA, Krawinkler H. 2005. "Hysteretic models that incorporate strength and stiffness deterioration." *Eq Eng Struct Dyn* 34 (12): 1489-1511.

Iervolino I, Manfredi G, Cosenza E. 2006. "Ground motion duration effects on nonlinear seismic response." *Eq Eng Struct Dyn* 35 (1): 21–38.

Karsan ID, Jirsa JO. 1969. "Behavior of concrete under compressive loading." *J Struct Div* 95 (ST12).

Kashani MM. 2014. *Seismic Performance of Corroded RC Bridge Piers: Development of a Multi-Mechanical Nonlinear Fibre Beam-Column Model.* PhD Thesis, Bristol: University of Bristol .

Kashani MM, Barmi AK, Malinova VS. 2015b. "Influence of inelastic buckling on low-cycle fatigue degradation of reinforcing bars." *Constr Build Mater* 644-655.

Kashani MM, Lowes LN, Crewe AJ, Alexander NA. 2014. "Finite element investigation of the influence of corrosion pattern on inelastic buckling and cyclic response of corroded reinforcing bars." *Eng Struct* 113-125.

Kashani MM, Lowes LN, Crewe AJ, Alexander NA. 2016. "Nonlinear fibre element modelling of RC bridge piers considering inelastic buckling of reinforcement." *Eng Struct* 116: 163-177.

Kashani MM, Lowes LN, Crewe AJ, Alexander NA. 2015a. "Phenomenological hysteretic model for corroded reinforcing bars including inelastic buckling and low-cycle fatigue degradation." *Comput Struct* 58-71.

Kramer SL. 1996. *Geotechnical earthquake engineering.* Vol. 80. Upper Saddle River, NJ: Prentice Hall.

Kunnath SK, El-Bahy A, Taylor AW, Stone WC. 1997. *Cumulative seismic damage of reinforced concrete bridge piers.* Technical Report NCEER .

Lehman DE, Moehle JP. 2000. *Seismic performance of well-confined concrete bridge columns.* Berkeley: Pacific Earthquake Engineering Recerch Centre.

Málaga-Chuquitaype C. 2015. "Estimation of peak displacements in steel structures through dimensional analysis and the efficiency of alternative ground-motion time and length scales." *Engineering Structures* 101: 264-278.

Mander JB, Panthaki FD and Kasalanat A. 1994. "Low-cycle fatigue behavior of reinforcing steel." *J Mater Civil Eng* 6 (4): 453–468.

Mander JB, Priestley MJN, Park R. 1988. "Theoretical stress-strain model for confined concrete." *J Struct Eng* 114 (8): 1804-1825.

Menegotto M, and Pinto PE. 1973. "Method of analysis of cyclically loaded RC plane frames including changes in geometry and nonelastic behavior of elements under normal force and bending." In *Preliminary Report*, 13:15–22. Zurich: IABSE.

Neuenhofer A, Filippou FC. 1998. "Geometrically nonlinear flexibility-based frame finite element." *J Struct Eng* 124 (6): 704-71.

OpenSees. 2013. “The Open System for Earthquake Engineering Simulation,.” PEER, University of California, Berkeley.

PEER. 2010. *Guidelines for Performance-Based Seismic Design of Tall Buildings.* PEER 2010/05, Berkeley: Pacific Earthquake Engineering Research Center.

Popovics S. 1973. “A numerical approach to the complete stress strain curve for concrete.” *Cem Concr Res* 3 (5): 583-599.

R2013b, MTLAB. 1994-2012. “The MathWorks lnc.” www.mathworks.com.

Raghunandan M, Liel AB. 2013. “Effect of ground motion duration on earthquake-induced structural collapse.” *Struct Safe* 41: 119–133.

Sarieddine M, Lin L. 2013. “Investigation Correlations between Strong-motion Duration and Structural Damage.” *Structures Congress 2013.* Reston: American Society of Civil Engineers. 2926–2936.

Somerville PG, Smith NF, Graves RW, Abrahamson NA. 1997. “Modification of empirical strong ground motion attenuation relations to include the amplitude and duration effects of rupture directivity.” *Seismological Research Letters* 68 (1): 199-222.

Spacone E, Filippou FC, Taucer FF. 1996. “Fibre beam-column model for non-linear analysis of R/C frames: part I: formulation.” *Earthq Eng Struct D* 25: 711-725.

Spacone E, Filippou FC, Taucer FF. 1996. “Fibre beam-column model for non-linear analysis of R/C frames: part II: applications.” *Earthq Eng Struct D* 25: 727-742.

Uriz P. 2005. *Towards earthquake resistant design of concentrically braced steel structures.* University of California Berkeley,PhD Thesis.

Vamvatsikos D, Cornell CA. 2002. “Incremental dynamic analysis.” *Earthq Eng Struct D* 491-514.